Supporting information

Thermal Rectification and Thermal Logic Gates in Graded Alloy Semiconductors

Ryan C. Ng [1,*], Alejandro Castro-Alvarez [2,*], Clivia M. Sotomayor-Torres [1,3] and Emigdio Chávez-Ángel [1,*]

[1] Catalan Institute of Nanoscience and Nanotechnology (ICN2), CSIC, and BIST, Campus UAB, Bellaterra, 08193 Barcelona, Spain; clivia.sotomayor@icn2.cat
[2] Centro de Excelencia en Medicina Traslacional, Laboratorio de Bioproductos Farmacéuticos y Cosméticos, Facultad de Medicina, Universidad de La Frontera, Av. Francisco Salazar 01145, Temuco 4780000, Chile
[3] ICREA—Institució Catalana de Recerca i Estudis Avançats, 08010 Barcelona, Spain
* Correspondence: ryan.ng@icn2.cat (R.C.N.); alejandro.castro.a@ufrontera.cl (A.C.-A.); emigdio.chavez@icn2.cat (E.C.-Á.)

The COMSOL parameters for the thermal properties of the materials studied here are summarized in **Table S1**.

Table S1. Summary of COMSOL parameters.

Parameter	Value
α_{Si}	-1.3
α_{Ge}	-1.25
k_{Si}	150 [W/K/m]
k_{Ge}	60 [W/K/m]
α_{GaAs}	-1.25
α_{InAs}	-1.2
k_{GaAs}	46 [W/K/m]
k_{InAs}	27.3 [W/K/m]
α_{AlAs}	-1.37
k_{AlAs}	80 [W/K/m]

Table S1 summarizes the thermal parameters that are used in the COMSOL simulations for the materials studied here, where the parameters are defined in the main text.

Figure S1 shows the temperature (*a*-*e*) and thermal conductivity (*f*-*j*) distribution as a function of normalized position along a $Si_{(1-x)}Ge_x$ alloy rectifier slab. The T and k distributions were plotted for the x-concentrations that showed the largest R-factor for the Fermi-like, quadratic, and linear distributions. For the exponential and Gaussian distributions, the content varies from $0 < x < 0.9$, which is approximately the regime where $R > 1$.

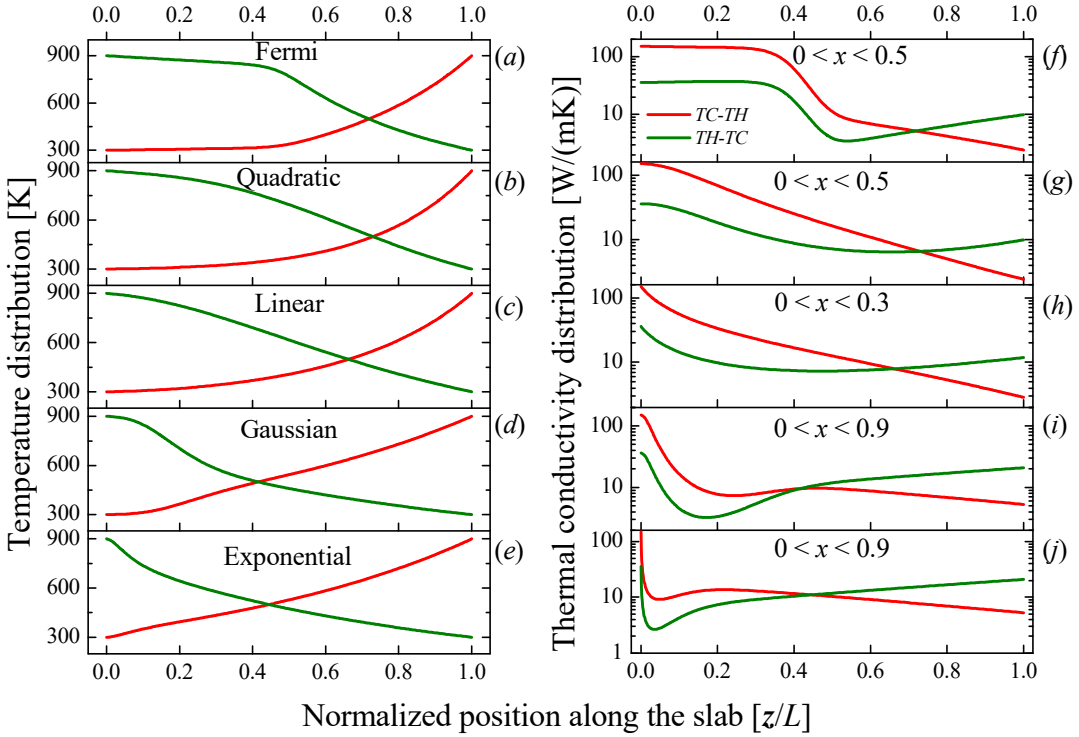

Figure S1. (***a-e***) *Temperature and* (***f-j***) *thermal conductivity distribution along the alloy slab for Fermi* (***a*** *and* ***f***)*, quadratic* (***b*** *and* ***g***)*, linear* (***c*** *and* ***h***)*, Gaussian* (***d*** *and* ***i***) *and exponential* (***e*** *and* ***j***) *Ge-content distributions.*

The spatial atomic distributions along the alloy $A_{(1-x)}B_x$ slab with a width L were generated using the following equations:

Linear

$$A-content=(1-(z/L)) \tag{1}$$

Quadratic

$$A-content=(1-(z/L)^2) \tag{2}$$

Exponential

$$A-content=\exp(-a_0 z/L) \tag{3}$$

Gaussian

$$A-content=\exp(-a_0(z/L)^2) \tag{4}$$

Fermi-like

$$A-content=1-\frac{1}{1+\exp(-3a_0(z/L-z_1))} \tag{5}$$

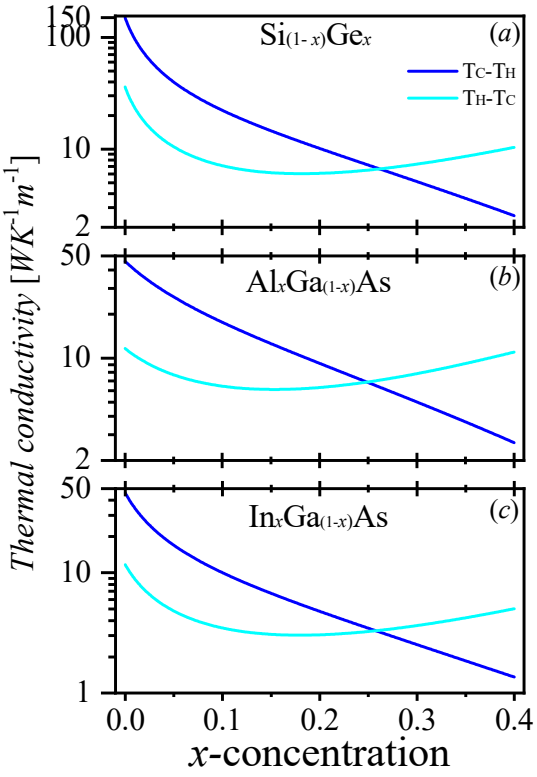

Figure S2. Thermal conductivity distributions for a linear distribution of alloy in (**a**) $Si_{(1-x)}Ge_x$, (**b**) $Al_xGa_{(1-x)}As$, and (**c**) $In_xGa_{(1-x)}As$.

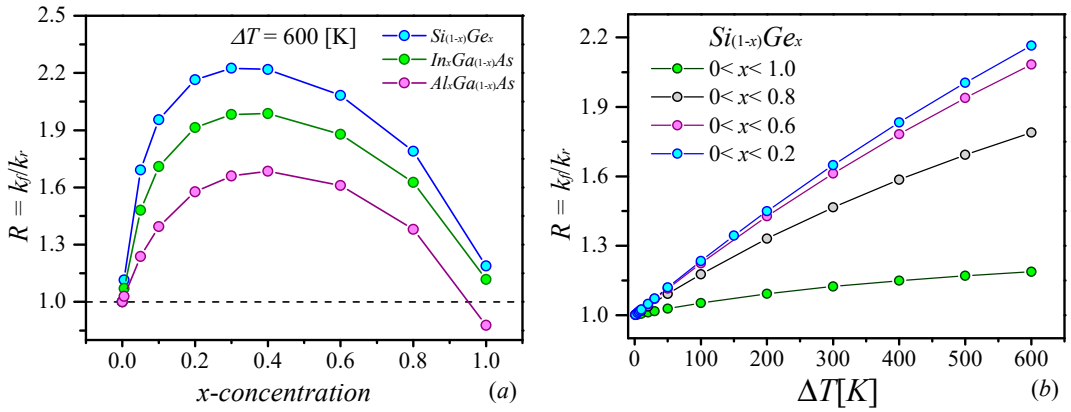

Figure S3. (**a**) Comparison of rectification as a function of x in each alloy material for $\Delta T = 600$ [K]. (**b**) Impact of the temperature rise on rectification factor for a four linear mass distribution in SiGe alloy.

Figure S2 shows the distribution for the thermal conductivity in various alloys for an alloy composition that is linearly varied across the slab for both the forward and reverse configurations. In general, the highest thermal conductivity is in the $Si_{(1-x)}Ge_x$ alloy. We can then compare the rectification between these three alloys (**Figure S3a**. While the $Si_{(1-x)}Ge_x$ alloy has the greatest rectification due to the higher k, we note that the qualitative trend is the same between all alloys, allowing the results of this work to be readily extended to other graded alloys by primarily considering k_{AB}. **Figure S3b** shows the dependence of the rectification factor with respect to the temperature rise ($\Delta T = T_H - T_C$) for four different linear mass distribution in $Si_{(1-x)}Ge_x$ alloy system.

where a_0 is an arbitrary number to fix the decay of the exponential expressions in Eq. (3) and (4) and the smoothness of (5), and z_1 is the position which sets the half point of the Fermi distribution.

In this work we fixed $a_0 = L$ and z_1 was varied from 10 to 80% along the normalized position of the slab.

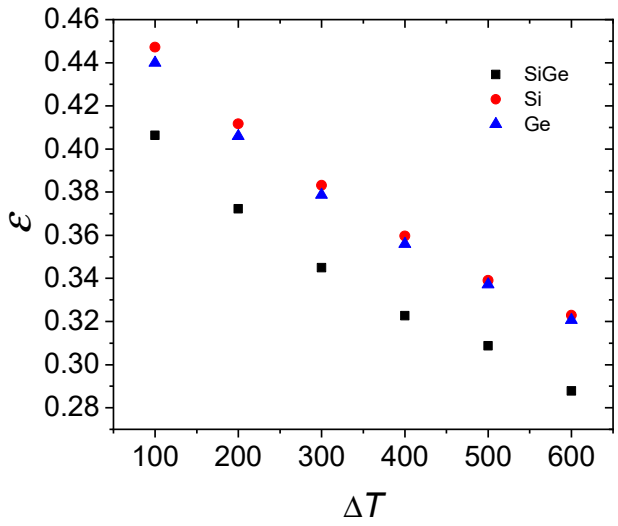

Figure S4. Comparison of the effectiveness, ε, as a function of ΔT for pure Si, pure Ge, and an alloy of SiGe.

We can also compare the effectiveness, ε, as a function of ΔT for pure Si, pure Ge, and an alloy of SiGe (**Figure S4**). We note that in the case of the SiGe alloy, we can reach much lower values of ε, which is useful for setting the threshold for our "low" output.

Table S2. Truth table for an AND-gate based on a pure Si slab.

T_A [K]	T_B [K]	T_{out} [K]	Input A	Input B	Output, ε
300	900	493.54	0	1	0.323
900	300	493.54	1	0	0.323
300	300	300	0	0	0
900	900	885.08	1	1	0.975

Table S3 Truth table for an AND-gate based on a pure Ge slab.

T_A [K]	T_B [K]	T_{out} [K]	Input A	Input B	Output, ε
300	900	492. 4	0	1	0.321
900	300	492.4	1	0	0.321
300	300	300	0	0	0
900	900	866.16	1	1	0.944